Effect of Modified Layered Silicates and Compatibilizer on Properties of PMP/Clay Nanocomposites

Santosh D. Wanjale, J.P. Jog

Chemical Engineering Division, National Chemical Laboratory, Dr. Homi Bhabha Road, Pune 411 008, India

Received 22 April 2002; accepted 7 April 2003

ABSTRACT: The preparation and properties of poly(4-methyl-1-pentene) (PMP)/clay nano-composites are described for the first time. The effect of clay modification and compatibilizer on the formation and properties of the nanocomposites is studied. Layered silicates modified with two types of quaternary ammonium salts are used. The X-ray diffraction results indicate intercalation of the polymer into the intergallery spacing of the clay. Thermogravimetric analysis shows a delay in the degradation process. Dynamic mechanical analysis shows an increase in the storage modulus for the nanocomposites. The use of compatibilizer containing maleic anhydride and acrylic ester groups is explored. © 2003 Wiley Periodicals, Inc. J Appl Polym Sci 90: 3233–3238, 2003

Key words: nanocomposites; modulus; compatibilization; thermogravimetric analysis (TGA)

INTRODUCTION

Recently, nanocomposites based on organophilic clays are increasingly being developed and studied because of their unique combinations of properties. The preparation of a nanocomposite involves the intercalation of polymer into organophilic clay layers via *in situ* polymerization, solution or melt intercalation. Of these three techniques, melt intercalation is an obvious choice for a wide range of polymers. The expansion of intergallery spacing takes place depending on the polymer/clay interactions. The process of intercalation is favored in the case of polar polymers due to the interaction with the hydroxyl groups of the silicate layers. However, the hydrophilic layered silicates are intrinsically incompatible with most polymers (especially nonpolar polymers); thus the dispersion of the silicate layers or the insertion of polymer into the silicate layers is very difficult. In such cases, the inorganic cations in the galleries of the pristine clay are exchanged for tallow compounds/surfactants, which make the clay organophilic and compatible with the polymer. Another method is the use of a third component (with polar groups, like maleic anhydride) to promote the intercalation of polyolefins. The dispersion of the clay into the polymer matrix at nanometer-scale leads to significant improvements in the composites' thermal, mechanical and barrier properties.[1–7] These new materials can satisfy the demanding requirements of materials for high technology applications.

Correspondence to: J. Jog (email: jyoti@che.ncl.res.in).

Journal of Applied Polymer Science, Vol. 90, 3233–3238 (2003)

Poly(4-methyl-1-pentene) (PMP) is a member of the polyolefin family. It is used in a variety of applications, such as automotive components, light covers, pacemaker parts, blood collection and transfusion devices and others. The special properties of interest with regard to polyolefins are low density, high thermal stability, chemical resistance, optical transparency and high permeability. However, the applications of these polymers are limited, as their mechanical properties deteriorate even at temperatures just above room temperature.

In this article, we present the results of our study of the preparation and properties of PMP/clay nanocomposites. Due to the hydrophilic nature of pristine clay, it is difficult to achieve intercalation of a non polar polymer in silicate layers. The organically modified clays used for the present investigation consist of long hydrocarbon chains, which make the clay surface less hydrophilic and thus favor intercalation of the polymer. A polyolefin-based polymer with polar groups, such as maleic anhydride, is used as compatibilizer because it is known to react with the clay surface, resulting in better interfacial properties[8] to further assist the intercalation process. The melt intercalation of organophilic clay is carried out using a Brabender Plasticorder. The nanocomposites are characterized using X-ray diffraction (XRD), dynamic mechanical analysis (DMA) and thermo gravimetric analysis (TGA).

EXPERIMENTAL

Materials

PMP with a melt flow index (MFI) of 8, procured from Aldrich (Milwaukee, WI), was used in the present

TABLE I
Codes and Compositions of Samples

Code	Composition
P	PMP
P6	PMP + 3% 6A
P6C	PMP + 3% 6A + 9% Lotader 3700
P25	PMP + 3% 25A
P25C	PMP + 3% 25A + 9% Lotader 3700
PC	PMP + 9% Lotader 3700

investigation. The organically modified clay samples, Cloisite® 6A [a dimethyl, dihydrogenated tallow, quaternary ammonium chloride treated bentonite clay with cation exchange capacity (CEC) of 140 mEq/100g], and Cloisite® 25A, [a dimethyl, dihydrogenated tallow, 2-ethyl-hexyl quaternary ammonium methyl sulfate treated bentonite clay with CEC of 125 mEq/100g] were generously donated by Southern Clay Products (Gonzales, TX). The alkyl ammonium ions reduce the attractive forces between the clay layers and help in the intercalation of the polymer. The organic content was 47 and 34% for clays 6A and 25A respectively. The mineral content in the nanocomposites, however, differed due to surfactant present in the treated clays. The 6A clay was more hydrophobic than the 25A, according to the company data sheet. It was therefore expected that the nanocomposites prepared using these two clays would exhibit variation in their structure and properties.

A polyethylene based compatibilizer, Lotader3700, was procured from CDF Chimie, Paris, France. It was a terpolymer of ethylene, acrylic ester and maleic anhydride with a comonomer content of about 32%. Its MFI value was 5 at 190°C/2.16kg, and its melting point was 67°C, according to the company data sheet.

Melt Compounding

The melt compounding of PMP with the clays was carried out using a Brabender Plasticorder at 250°C at 50 rpm for 3 min. The clay samples were dried in an air circulatory oven at 60°C for 8 h prior to compounding.

Two compositions, containing 3% (wt/wt) clay with and without compatibilizer were prepared from 6A and 25A clay. All of the ingredients were mixed simultaneously. A blend of PMP with 9% compatibilizer was prepared in the same way as the other composites. Sample codes and compositions are presented in Table I. The inorganic content for the nancomposites was 1.6 and 1.9% for 6A and 25 A respectively.

The XRD and DMA were completed on compression-molded films of the nanocomposites prepared using Carver press model F - 15181 at 250°C with nominal pressure.

X-Ray Diffraction

The structure of the nanocomposites was evaluated using XRD measurements. Rigaku X-ray diffractometer model Dmax 2500 with Cu K_α radiation ($\lambda = 0.154$ nm) operated at 40 kV and 150 mA was used. The samples were scanned from 2 to 15° in 2θ. The basal spacing of the clay was estimated from the d_{001} peak in the XRD pattern.

Thermo Gravimetric Analysis

TGA was done using Perkin Elmer thermal analysis system model TGA 7. The TGA scans were recorded at a heating rate of 10°C/min under nitrogen atmosphere in the temperature range of 50 to 600°C.

Dynamic Mechanical Analysis

Dynamic mechanical properties of the samples were studied on compression-molded films using Rheometrics Dynamic Mechanical Analyzer model IIIE, in the tensile mode. The samples were tested in a temperature range from −40 to 150°C at a frequency of 10 rad/s and 0.05% strain. The temperature sweep was carried out in auto strain mode.

RESULTS AND DISCUSSION

XRD of PMP/clay nanocomposites

The process of melt intercalation of polymer into silicate layers is schematically shown in Figure 1. The nanocomposite structure can be classified broadly into two types, namely intercalated (finite layer expansion) and exfoliated (delamination). However, in practice, a combination of intercalated and exfoliated structures is most commonly obtained. The structure of the nanocomposites can be determined using XRD techniques from the position, shape and the intensity of the basal reflections in the XRD patterns. Figure 2 shows the XRD patterns for the 6A clay and its nanocomposites. The XRD pattern of 6A clay shows three characteristic peaks at basal spacings of 3.3 nm, 1.8 nm and 1.2 nm corresponding to d_{001}, d_{002} and d_{003} respectively. As can be seen from the figure, nanocomposites show remarkable differences in X-ray patterns from those of

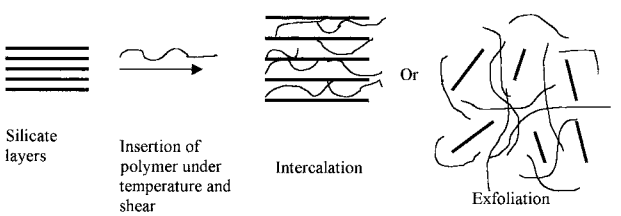

Figure 1 Schematic presentation of intercalation of polymer into silicate layers.

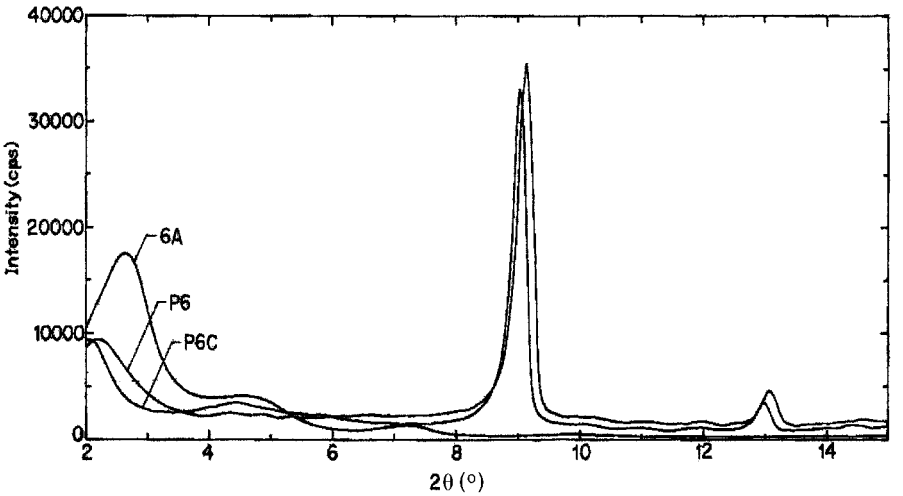

Figure 2 XRD pattern for 6A clay, P6 and P6C nanocomposites.

pure clay. The d_{001} peak is shifted to a lower angle, corresponding to a d-spacing of 4.0 nm, and some higher order peaks are also observed. The increase in the d_{001} spacing is about 0.7 nm. As reported earlier,[9] the shift in the d_{001} peak to a lower angle can be attributed to an intercalated structure of the clay layers in the nanocomposite. The presence of higher order peaks shows that the ordered structure of the layers is not disrupted due to the intercalation of the polymer.

Figure 3 shows the XRD pattern for the 25A clay and the P25 and P25C nanocomposites. The XRD pattern of 25A clay shows one characteristic peak corresponding to a basal spacing of 1.8 nm. As can be seen from the figure, the nanocomposite shows two broad peaks at d-spacings of 3.2 nm and 1.5 nm, indicating a shift of about 1.4 nm. The broadening of the peaks suggests that the intercalation of polymer into the layered structure has taken place, leading to a disordered structure of the layers.

The differences observed in the structures of the two nanocomposites, P6 and P25, is presumably due to the different extent of interaction of polymer with intercalant used in modifying the clays.

Dynamic Mechanical Analysis

The most significant property improvement in the nanocomposites is observed in the dynamic storage modulus of the polymer. This observation is related to the dispersion of clay layers in polymer matrix. The intercalation of the polymer into silicate layers first leads to the breaking of the primary clay particles into smaller tactoids. As the degree of intercalation increases, the clay layers are set apart farther and farther, thus apparently increasing the aspect ratio of the layers. Both the degree of intercalation and the aspect ratio affect the ultimate properties of the nanocomposites.

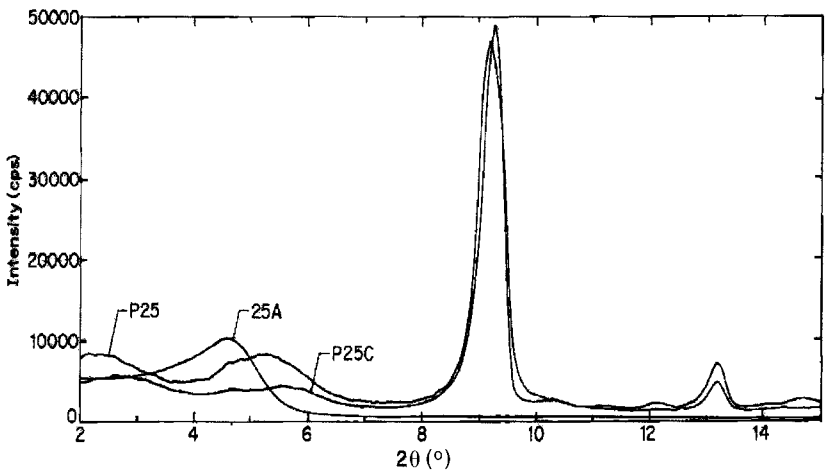

Figure 3 XRD patterns for 25A clay, P25 and P25C nanocomposites.

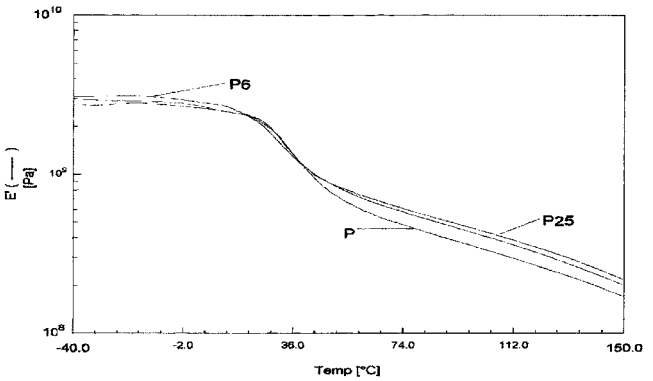

Figure 4 Storage modulus for P, P6 and P25 nanocomposites.

Figure 4 depicts the DMA scans of sample P and its nanocomposites. It can be seen from the figure that P exhibits a storage modulus of 2.7281 GPa at −40°C, which decreases with temperature, and at 150°C it reaches a value of 0.17056 GPa. The sharp decrease in the storage modulus above 25°C corresponds to the onset of micro-Brownian motion in the polymer. The tan δ peak at 37°C represents the glass transition temperature (T_g) of the polymer and is associated with the motions of the long chain segments in the amorphous region of the polymer. This value of T_g is in good agreement with the reported values of T_g for PMP, which are found to vary between 18 and 45°C, depending on the technique of measurement.[11–14]

In the glassy state, both of the nanocomposites (P6 and P25) exhibit only a 10% increase in the storage modulus. However, as the temperature increases, the reinforcing effect of the clay layers becomes discernible. At high temperatures from 40 to 150°C, an increase of 20 and 30% is observed in the modulus for hybrids P6 and P25, respectively. It is noteworthy that the effect of the clay layers becomes operative above the T_g of P. The improvement in the modulus is presumably due to the interaction of clay layers with the polymer, leading to improved interfacial properties. A similar increase in storage modulus was reported earlier in case of other nanocomposites.[15–19] The tan δ peak is found to shift slightly to lower temperatures in nanocomposites P6 and P25.

In the case of P, it is reported that,[20] in dynamic mechanical studies, two transitions are observed, one at 20–50°C, corresponding to chain motion in the amorphous region, and another at 105–135°C, corresponding to chain motion in the crystalline region. Each of these transitions is accompanied by a drop in the shear modulus by a factor of 5. In our studies of DMA with tensile mode, we observed only one transition at 37°C, corresponding to the T_g. The drop in tensile modulus for P by a factor of 4.5 at 60°C was noted, whereas for nanocomposites P6 and P25 it was observed that the factor decreased to 3.8 and 3.6, respectively. This clearly indicates a comparatively lesser drop in modulus at higher temperatures.

Effect of Compatibilizer

In non polar polymer/clay nanocomposites, the use of a compatibilizer has been found to result in better intercalation and dispersion of clay layers in the polymer.[8] Due to the presence of polar groups in the compatibilizer, the interaction between the clay and the polymer can be further enhanced. In the present case, as shown in Figure 2, the addition of compatibilizer is found to result in an additional increase in d-spacing for P6C, whereas in the case of P25C nanocomposites, a significant reduction in the intensity and broadening of the peaks is observed. The increase in d-spacing observed in P6C indicates the intercalation of polymer without significant disruption of the layer structure of the clay. However, in case of P25C, the

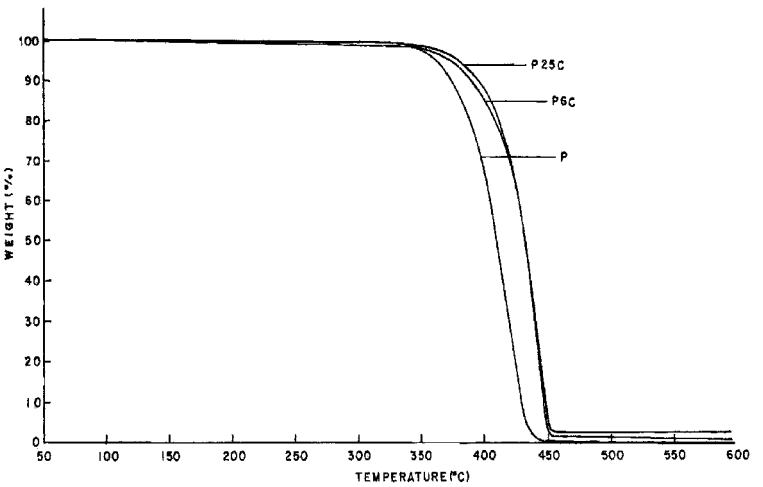

Figure 5 TGA thermogram for P, P6C and P25C nanocomposites.

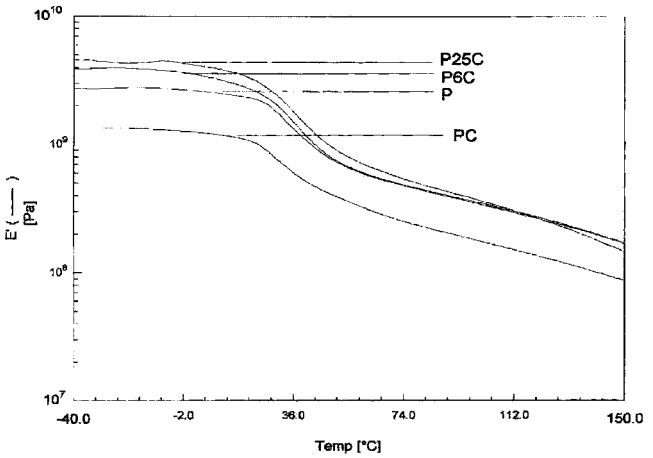

Figure 6 Storage modulus for P, PC, P6C and P25C nanocomposites.

XRD pattern of broad peaks with much reduced intensity indicates the intercalation of polymer with significant disruption of the layer structure of the clay.

The incorporation of clay in a platelet form is known to result in the improvement of the thermal stability of polymers.[21–23] Figure 5 depicts the TGA scans of P and compatibilized nanocomposites, recorded under nitrogen. In the case of P6 and P25, there is a marginal increase in the onset-of-degradation temperature, by 8 and 10°C respectively. On the other hand, in the case of compatibilized nanocomposites, the temperature at which 10% weight loss occurred is found to increase by 13 and 16°C for P6C and P25C with respect to P, while for 50% weight loss it is found to increase by 28°C. It is also observed that the degradation peak increased by 20°C in P6C and P25C. In the case of compatibilized nanocomposites, a temperature lag of 28°C observed could be ascribed to better dispersion or adhesion of silicate layers, which inhibit the weight loss of P. Similar increase has been observed in case of polypropylene/clay/compatibilizer nanocomposites.[24]

Figure 6 depicts the temperature dependence of the storage modulus of blend PC and nanocomposites. The relative storage moduli of nanocomposites at various temperatures are presented in Table II. It can be seen from the table that at −30°C (below the T_g of P), the addition of compatibilizer results in a significant increase of storage modulus for both nanocomposites. For P6C, the relative modulus increases from 1.15 to 1.48, whereas for P25C the relative storage modulus increases from 1.10 to 1.73. Thus an increase of 48% for P6C and 73% for P25C with respect to P is obtained as a result of the addition of compatibilizer. Even at room temperature, the moduli of P6C and P25C are higher than those of P6 and P25. However, at higher temperatures, the storage moduli for P6C and P25C are less than those for P6 and P25. This observation is attributed to the softening of the compatibilizer at higher temperatures (melting point of compatibilizer = 67°C). This contention is supported by the fact that the blend PC exhibits lower modulus than the pristine polymer over the entire temperature range.

The incorporation of fillers is known to enhance the moduli of the composites. This enhancement is dependent on the filler volume fraction and the aspect ratio of the filler. The effect of the aspect ratio of the filler on the modulus can be estimated using a modification of Guth's equation, used to describe the modulus of composites containing non-spherical fillers. The dependence of dynamic storage modulus on volume fraction of filler can be predicted by taking into account the aspect ratio of the filler and can be expressed as

$$E_c = E_m(1 + 0.67 f_g v_f + 1.62 f_g^2 v_f^2)$$

where E_c is the modulus of the composite, E_m is the modulus of the matrix, f_g is the ratio of filler particle length to width or the apparent aspect ratio (for spherical fillers, the value of f_g would be 1), and v_f is the filler volume fraction.[25] The apparent aspect ratios of the clay particles in the nanocomposites were calculated using Guth's equation. For P6 and P6C samples, the apparent aspect ratios are 12 and 26, respectively, while for P25 and P25 C they are 9 and 37 respectively. The calculated values of the apparent aspect ratios suggest that the filler is not in spherical form but in platelet form (which exhibits a higher aspect ratio). The higher values of the apparent aspect ratio for P6C and P25 C as compared to P6 and P25 imply that the clay particles are dispersed in a platelet form (higher

TABLE II
Relative Dynamic Storage Modulus at Various Temperatures for Nanocomposites

Sample	Temperature (°C)					Tan δ Peak Temperature (°C)
	−30	0	30	70	100	
P6	1.15	1.09	0.85	1.19	1.22	31
P6C	1.48	1.36	1.10	1.01	1.03	36
P25	1.10	1.05	0.98	1.25	1.30	34
P25C	1.73	1.63	1.35	1.15	1.06	37
PC	0.51	0.48	0.41	0.52	0.52	33

aspect ratio) in the presence of compatibilizer. The observed increase in the storage modulus of the nanocomposites can thus be ascribed to the increased apparent aspect ratio of the clay in the presence of compatibilizer.

In summary, it was found that, by the addition of compatibilizer, the dispersion of clay layers can be improved in the polymer matrix, as evidenced by XRD patterns, increased modulus and increased degradation temperature. However, the improvement in the storage modulus at high temperature is unsatisfactory due to the softening of the compatibilizer.

CONCLUSIONS

Nanocomposites of PMP and clay were successfully prepared using a melt intercalation technique. Two organophilic clays were used to facilitate intercalation of the polymer. From the XRD results, one can conclude that, for both types of clays, the structures of the nanocomposites formed are intercalated, disordered and/or partially exfoliated. DMA illustrates the reinforcing effect of clay, as evidenced by the improved storage modulus over a range of temperatures studied. The effect of clay treatment on nanocomposite is discernible in the dynamic response of the nanocomposites. The extent of increase in storage modulus is significantly higher for nanocomposites prepared using 25A clay and compatibilizer than that of 6A clay based nanocomposite. In the present case, 6A clay has larger d-spacing and is more hydrophobic than 25A; nevertheless; the results show that the nanocomposites with 25A clay exhibit better properties. The addition of compatibilizer results in increased d-spacing, and improved thermal stability but does not bring about much improvement in the dynamic storage modulus at higher temperatures (due to the low melting point of the compatibilizer). From this observation, it can be concluded that, by choosing a compatibilizer with a high softening/melting point, a good combination of properties with respect to the pristine polymer can be achieved.

The authors would like to thank the Department of Science and Technology, New Delhi, India for financial support.

References

1. Vaia, R. A.; Ishii, H.; Giannelis, E.P. Chem Mater 1993, 5, 1694.
2. Jimenez, G.; Ogata, N.; Kawai, H.; Ogihara, T. J Appl Polym Sci 1997, 64, 2211.
3. Messersmith, P. B.; Giannelis, E.P. Chem Mater 1994, 6, 1719.
4. Liu, L.; Qi, Z.; Shu, X. J Appl Polym Sci 1999, 71, 1133.
5. Usuki, A.; Kojima, Y.; Kawasumi, M.; Okada, A.; Fukushima, Y.; Kurauchi, T.; Kamigaito, O. J Mater Res 1993, 8, 1185.
6. Zilg, C.; Mulhaupt, R.; Finter, J. Macromol Chem Phys 1999, 200, 661.
7. Ijdo, W. L.; Pinnavaia, T. J. Solid State Chem 1998, 139, 281.
8. Kawasumi, M.; Hasegawa, N.; Kato, M.; Usuki, A.; Okada, A. Macromolecules 1997, 30, 6333.
9. Vaia, R. A.; Giannelis, E. P. Macromolecules 1997, 30, 8000.
10. Zollar, P.; Howard, W.; Starkweather, J.; Jones, G. A. J Polym Sci Part B: Polym Phys 1986, 24, 1451.
11. Griffith, J. H.; Ranby, B. G. J Polym Sci 1960, XLIV, 369.
12. Ranby, B. G.; Chan, K. S.; Brumberger, H. J Polym Sci 1962, 58, 545.
13. Zoller, P. J Appl Polym Sci 1997, 21, 3129–3137.
14. Hartmann, B. J Appl Phys 1980, 51, 310.
15. Usuki, A.; Kojima, Y.; Kawasumi, M.; Okada, A.; Fukushima, Y.; Kurauchi, T.; Kamigaito, O. J Mater Res 1993, 8, 1179.
16. Yano, K.; Usuki, A.; Kurauchi, T.; Kamigaito, O. J Polym. Sci Part A: Polym Chem 1993, 31, 2493.
17. Kodgire, P.; Kalgaonkar, R.; Hambir, S.; Bulakh, N.; Jog, J. P. J Appl Polym Sci 2001, 81, 1786.
18. Hambir, S.; Bulakh, N.; Kodgire, P.; Kalgaonkar, R.; Jog, J. P. J Polym Sci Part B: Polym Phys 2001, 39, 446.
19. Huang, J.; Zhu, Z.; Yin, J.; Qian, X.; Sun, Y. Polymer 2001, 42, 873.
20. Reddy, S.; Desai, P.; Abhiraman, A.; Beckham, H.; Kulik, A.; Spiess, H. Macromolecules 1997, 30, 3293.
21. Noh, H. W.; Lee, D. C. Polym Bull 1999, 42, 61.
22. Burnside, S. D.; Giannelis, E. P. Chem Mater 1995, 7, 1597.
23. Wang, Z.; Pinnavaia, T. J. Chem Mater 1998, 10, 1820.
24. Hambir, S.; Bulakh, N.; Jog, J. P. Polym Eng Sci 2002, 42, 1800.
25. Dufresne, A.; Cavaille, J. J Polym Sci Part B: Polym Phys 1998, 36, 2211.